Confined carbon mediating dehydroaromatization of methane over Mo/ZSM-5

Zeolites

Deutsche Ausgabe: DOI: 10.1002/ange.201711098
Internationale Ausgabe: DOI: 10.1002/anie.201711098

Confined Carbon Mediating Dehydroaromatization of Methane over Mo/ZSM-5

Nikolay Kosinov, Alexandra S. G. Wijpkema, Evgeny Uslamin, Roderigh Rohling, Ferdy J. A. G. Coumans, Brahim Mezari, Alexander Parastaev, Artem S. Poryvaev, Matvey V. Fedin, Evgeny A. Pidko, and Emiel J. M. Hensen**

Abstract: *Non-oxidative dehydroaromatization of methane (MDA) is a promising catalytic process for direct valorization of natural gas to liquid hydrocarbons. The application of this reaction in practical technology is hindered by a lack of understanding about the mechanism and nature of the active sites in benchmark zeolite-based Mo/ZSM-5 catalysts, which precludes the solution of problems such as rapid catalyst deactivation. By applying spectroscopy and microscopy, it is shown that the active centers in Mo/ZSM-5 are partially reduced single-atom Mo sites stabilized by the zeolite framework. By combining a pulse reaction technique with isotope labeling of methane, MDA is shown to be governed by a hydrocarbon pool mechanism in which benzene is derived from secondary reactions of confined polyaromatic carbon species with the initial products of methane activation.*

The abundance of natural gas reserves calls for the development of an efficient conversion technology to upgrade its principal component, methane, into easily transportable chemicals.[1] Several catalytic technologies, which could replace the current indirect route involving an expensive synthesis gas generation step, are being considered. Broadly, we can distinguish between oxidative and non-oxidative direct routes.[2] Among the non-oxidative approaches, catalytic methane dehydroaromatization (MDA) is one of the most promising methods. After the initial reports on MDA almost three decades ago,[3] a substantial body of literature has appeared.[4] The industrial implementation of the MDA process is mainly hindered by rapid catalyst deactivation caused by the deposition of a carbonaceous material that blocks the catalytically active sites.[5] Although there have been remarkable achievements in regeneration procedures,[6] developing a stable MDA catalyst is still required to arrive at a commercial process. A progress in this direction is seriously hampered by limited understanding of the active sites in the benchmark Mo/ZSM-5 catalyst and the mechanism of methane conversion to benzene and hydrogen. Despite considerable debate on the nature of the active phase, there is a growing consensus that the active sites are confined as highly dispersed Mo species by the zeolite pores in working Mo/ZSM-5 catalysts and that Mo_2C nanoparticles on the external surface are inactive.[7] Concerning the reaction mechanism, most reports support a bifunctional pathway in which methane is activated and coupled to ethylene over Mo-carbide species, followed by ethylene aromatization over the zeolite Brønsted acid sites.[8]

Important challenges in gaining insight into these aspects are the high reaction temperature at which the MDA reaction takes place and its transient nature, which involves rapid activation and deactivation stages when the fresh Mo/ZSM-5 catalyst is exposed to a methane feed. These factors complicate operando spectroscopy and kinetic investigations. A valuable approach in this regard is to increase the temporal resolution by pulsing the reactant over the catalyst and to use recovered samples at different stages of the reaction for characterization with spectroscopic and microscopic tools.[9] In this work, we performed pulsed MDA reactions at 700 °C in combination with mass spectrometry (MS) to follow the progress of the reaction (Supporting Information, Figure S1), and this procedure was found to be highly reproducible (Supporting Information, Figure S3). For these tests, we employed a commercial HZSM-5 zeolite (Si/Al 13) with Mo loadings of 1 wt% (catalyst denoted as 1%Mo), 2 wt% (2%Mo), and 5 wt% (5%Mo). As Figure 1a demonstrates, we chose these catalysts to distinguish between the larger Mo clusters, which are abundant on the surface of 5%Mo, and dispersed Mo complexes located inside the zeolite pores, which are exclusively present in 1%Mo.[10] This discrimination is important as the Mo centers confined inside the pores catalyze the reaction, and larger, catalytically irrelevant, and generally more easily detectable species on the external surface often dominate during spectroscopy characterization.

The high-resolution pulse reaction method (Figure 1b–d) reveals that there are three distinct stages during the MDA reaction. The first stage corresponds to the slow reduction of the Mo phase, as characterized by the formation of carbon monoxide as the main carbon- and oxygen-containing product. We will refer to this as activation, and the duration of this stage correlates with the Mo loading. The second stage represents an induction period, when benzene formation starts and increases with every pulse until a constant benzene

[*] Dr. N. Kosinov, A. S. G. Wijpkema, E. Uslamin, R. Rohling, F. J. A. G. Coumans, B. Mezari, A. Parastaev, Dr. E. A. Pidko, Prof. E. J. M. Hensen
Laboratory of Inorganic Materials Chemistry
Eindhoven University of Technology
PO Box 513, 5600 MB Eindhoven (The Netherlands)
E-mail: N.A.Kosinov@tue.nl
E.J.M.Hensen@tue.nl
A. S. Poryvaev, Dr. M. V. Fedin
International Tomography Center SB RAS and
Novosibirsk State University
Novosibirsk 630090 (Russia)
Supporting information and the ORCID identification number(s) for the author(s) of this article can be found under: https://doi.org/10.1002/anie.201711098.

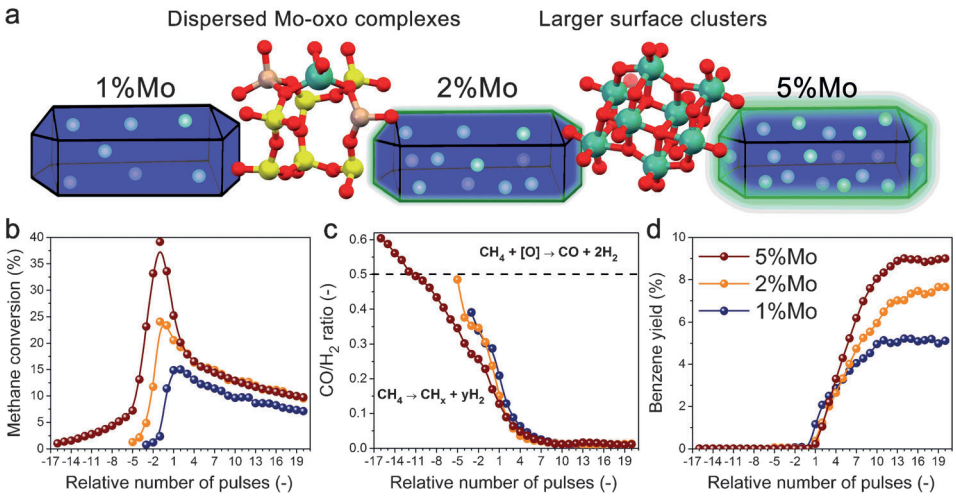

Figure 1. Representation of catalyst samples applied in this study, featuring exclusively atomically dispersed Mo^{VI} species stabilized in the zeolite pores for the 1%Mo sample and a mixture of the dispersed species and larger Mo-oxo clusters on the external surfaces of 2%Mo and 5%Mo catalysts (a). Per-pulse profiles of methane conversion (b), CO/H_2 ratio (c), and benzene yield (d), derived from MS analysis and recorded while pulsing 5 mL methane every 200 sec with 30 mL min^{-1} flow of Ar carrier.

yield is achieved. During this stage, the evolution of CO is negligible. For convenience, we assigned the pulse at which a benzene yield higher than 0.1% was observed as pulse number 1. It should be noted that the length of the induction period does not depend on the Mo loading; 10–15 methane pulses are required from the onset of benzene formation to achieve the maximum yield. Moreover, during the induction period, a significant amount of carbon is retained by the catalyst, as the yields of aromatics and carbon monoxide are low relative to the high conversion of methane (Figure 1b–d). Finally, the third stage is characterized by a stable production of benzene, followed by the usually observed gradual deactivation (Supporting Information, Figure S4). The occurrence of the three stages was confirmed by operando TGA experiments (Supporting Information, Figure S5), where the initial reduction of the Mo phase, the extent of which was highly dependent on the Mo loading, was followed by a rapid weight increase corresponding to deposition of carbon. On the basis of these observations it can be concluded that the activation stage corresponds to the removal of a certain amount of Mo-bound oxygen atoms, and during the induction period, mainly accumulation of surface carbon takes place.

To gain an insight into the evolution of the Mo species, we used operando X-ray absorption near-edge structure (XANES) spectroscopy. As Figure 2a and the Supporting Information, Figure S6 show, the XANES spectra of all three fresh catalysts show a significant pre-edge feature owing to tetrahedrally coordinated Mo species. For Mo/ZSM-5, this feature is attributed to Mo^{VI} monomers stabilized at the cationic exchange sites of the zeolite.[11] Upon pulsing methane, the Mo phase is reduced, as manifested by the disappearance of the pre-edge feature and the shift of the rising-edge feature to lower energy. We found it convenient to follow the reduction trend with ΔXANES (Figure 2b), where the main feature at 20.015 keV corresponds to the shifted and gradually increasing rising-edge feature. Figure 2c demonstrates the evolution of the 20.015 keV feature together with the benzene yield simultaneously determined. There is no correlation between the degree of Mo reduction and the induction period. In fact, the 1%Mo sample is only partially reduced as benzene formation sets in, whereas for 5%Mo, the induction starts after the Mo phase has been reduced. Two stages of Mo reduction can be distinguished: a fast reduction takes place during pulses 6–10 (more pulses for the higher Mo loading), and a slower one proceeds for a longer time and includes the reaction stage. Even after 30 pulses of methane, the intensity of the 20.015 keV feature continues to increase. A similar conclusion was drawn from an quasi-operando XPS analysis (Supporting Information, Figure S7). On the basis of the XANES, TGA, and XPS results, it can be concluded that the complete reduction of the active Mo species is not required for the formation of benzene to start.

To determine the dispersion of the active Mo phase, we performed a high-resolution high-angle annular dark-field scanning transmission electron microscopy (HAADF-STEM) study of the active catalysts at the end of the induction period. As Figure 2d demonstrates, we could not observe Mo particles on the 1%Mo-10 catalyst, although energy-dispersive X-ray (EDX) spectroscopy shows that Mo is homogeneously distributed in the catalyst. Although some agglomerated Mo was already seen on 2%Mo, images of 5%Mo show an abundance of Mo_2C particles (Supporting Information, Figure S9). A similar observation was made during TEM analysis of the catalysts, even after prolonged exposure (16 h) to methane at 700°C (Supporting Information, Figure S10). Furthermore, extended X-ray absorption fine structure spectroscopy analysis of these samples showed that there is no Mo–Mo coordination shell in the 1%Mo sample (Supporting Information, Figure S11 and Table S1). All of these findings point to the fact that active Mo species are atomically dispersed inside the pores of the working Mo/ZSM-5 catalysts. We propose (Figure 2e) that, during the activation and induction periods, the Mo centers anchored to the framework are partially reduced to yield single-atom active centers, which are slowly reduced further and can eventually detach from the Al-occupied oxygen tetrahedra of the zeolite.

Despite these extensive characterization data revealing important molecular-level details of the MDA reaction chemistry, the main question remains unanswered, namely what happens with the catalyst during the induction period. As, during the induction, methane is mostly consumed by the catalyst to form surface (hydro)carbon species, we asked ourselves whether such carbonaceous deposits play a role in

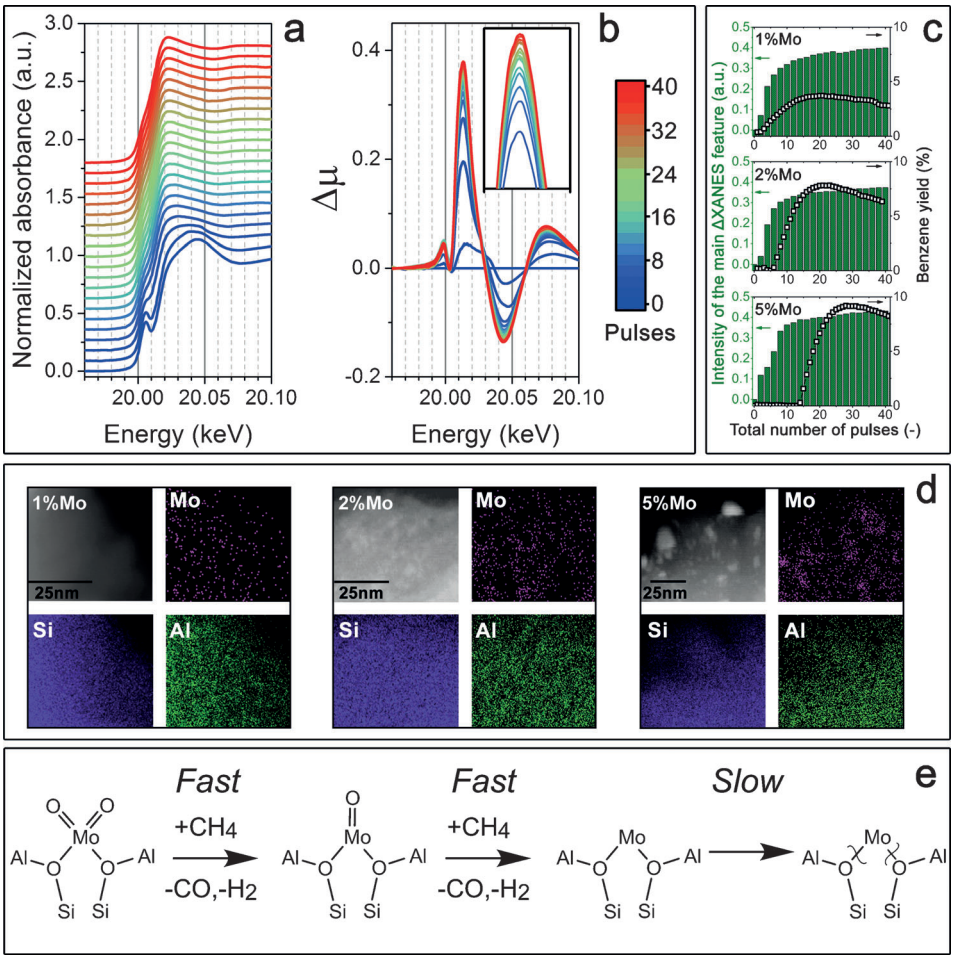

Figure 2. a) Operando Mo K-edge XANES spectra and b) corresponding ΔXANES spectra recorded while pulsing methane at 700 °C over the 2 %Mo catalyst. ΔXANES spectra were obtained using a spectrum recorded before pulsing methane as the background for subtraction. c) Comparison of the intensity of the main ΔXANES feature at 20.015 keV and the benzene yield values obtained simultaneously by MS analysis for 1 %Mo, 2 %Mo, and 5 %Mo catalysts. d) HAADF-STEM images and corresponding EDX elemental maps of Mo/ZSM-5 catalysts obtained with the catalysts quenched at the maximum benzene yield. e) Proposed evolution of the active Mo phase.

the catalytic mechanism. The concept of organocatalytic intermediates is well known in heterogeneous catalysis[12] and it has also been suggested for the MDA reaction by Jiang et al.[13a] and Kim et al.[13b] As clear experimental evidence for such a pathway was not provided, the organo-mediated nature of the MDA mechanism has not been widely considered.

To verify the role of confined carbon species in the MDA reaction, we expanded our characterization efforts to include Ar physisorption, nuclear magnetic resonance (NMR), and electron paramagnetic resonance (EPR) spectroscopy. Ar physisorption confirms that carbon mainly deposits inside the zeolite pores during the induction period, occupying 10–15 % of the micropore volume (Supporting Information, Figure S12). With the aid of ^{13}C NMR spectroscopy, we found that surface carbon is mainly of a polyaromatic nature as characterized by a broad peak centered at 128 ppm (Figure 3 a).[17] Furthermore, while the amount of carbon deposited on the catalysts during the induction period is similar, the C/Mo ratio varies from about 12 for 1 %Mo to about 4 for 5 %Mo, suggesting that confined carbon is not exclusively bound to Mo-species (Supporting Information, Figure S13, Table S2). We also found that the H/C ratio of surface carbon species is about 0.5, and that it remains constant during the reaction (Supporting Information, Figure S14). It is important to note that a Mo_2C signal at 272 ppm[18] was observed for the 2 %Mo and 5 %Mo samples (Supporting Information, Figure S15c). Together with the finding that Brønsted acid sites were not restored during the induction period, that is, Mo remained anchored to the zeolite framework (Supporting Information, Figure S15a,b), this result underpins our conclusion that Mo_2C species are merely spectators on the external surface and that the active Mo-species inside the pores are not carbidic in nature. Another indication of the structure and development of confined carbon species was obtained by EPR spectroscopy. Figure 3 b demonstrates the formation of a significant number of organic radicals on the 1 %Mo-10 catalyst, and the development of the concentration of radicals during the activation and induction stages (Figure 3 c) correlates well with the induction trend shown by Figure 1 d. A decrease of radical concentration between pulses 10 and 20 can be explained by the (inter-)growth of the confined hydrocarbon species, leading to a decrease of the number of perimeter carbon atoms.

To determine the catalytic relevance of the confined polyaromatic species, we combined our pulsing approach with isotopic labeling, using $^{13}CH_4$ and $^{12}CH_4$ pulses. Following the isotopologue distribution of formed benzene molecules provides insight into the involvement of carbonaceous species in the catalytic cycle. It is important to notice that between switching from one isotope to the other we thoroughly flushed the system with Ar flow at 700 °C to remove any volatile aromatics from the zeolite pores; therefore, the possibility of isotope scrambling between light aromatics and methane can be excluded. Figure 4 a shows that, after the induction period of 2 %Mo by $^{13}CH_4$ pulsing, the benzene product obtained after switching to $^{12}CH_4$ contains a significant amount of ^{13}C. In fact, more than 70 % of the benzene molecules, formed

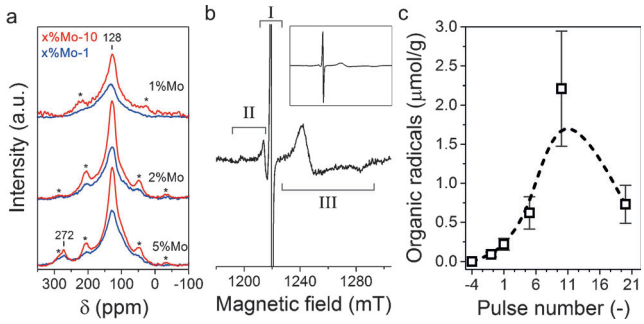

Figure 3. a) ^{13}C MAS NMR spectra of catalysts corresponding to the beginning and the end of the induction period. Samples for NMR were prepared using pure $^{13}CH_4$ to enhance the ^{13}C NMR signal. The spectra are normalized by the number of scans and sample weight. Asterisks denote spinning sidebands. b) Q-band EPR spectra of 1%Mo-10, featuring three signals: I-isotropic signal of aromatic radicals with $g=2.002$,[14] II-anisotropic signal corresponding to O-centered radicals within the zeolite with $g_{\perp}=2.009$ and $g_{\parallel}=2.037$ related to electron transfer from the framework to organic molecules,[15] III-anisotropic signal of Mo^{5+} centers with $g_{\perp}=1.964$ and $g_{\parallel}=1.903$.[16] See the Supporting Information, Figures S16–S18 for the EPR spectra of other samples and ENDOR spectrum of 1%Mo-10. c) Evolution of the concentration of organic radicals during the induction period over the 1%Mo catalyst.

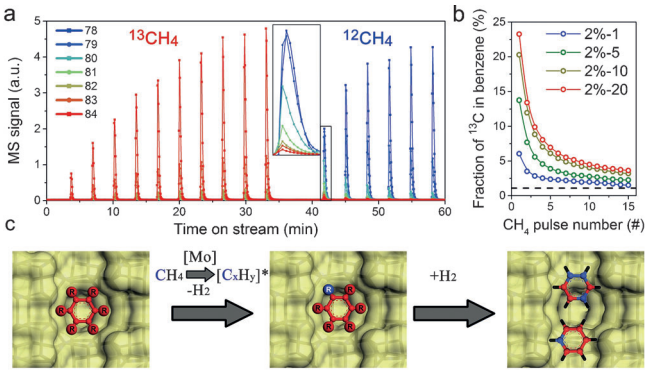

Figure 4. a) Results of pulsing isotopic exchange with $^{12}CH_4$ obtained after 10 pulses (relative number) of $^{13}CH4$ over 2%Mo. Complete profiles demonstrating the distribution of benzene isotopologues; a zoom in at the first pulse after the switch to $^{12}CH_4$ is shown in the inset. Isotope exchange experiments for 1%Mo and 5%Mo as well as the isotopologue distribution are shown in the Supporting Information, Figure S19. b) Development of ^{13}C incorporation into benzene with the number of $^{13}CH_4$ pulses (relative to the onset of benzene formation) over 2%Mo catalyst. The dashed line represents the 1.1% natural abundance of ^{13}C in $^{12}CH_4$. c) Proposed mechanism leading to benzene in the MDA reaction, depicting the aromatic nature of the confined carbon species. R substituents are mainly aromatic rings (^{13}C atoms are shown in red, ^{12}C atoms in blue, and protons in black).

after the first $^{12}CH_4$ pulse, contain at least one ^{13}C atom (Supporting Information, Figure S19). Importantly, we found that the degree of ^{13}C incorporation was the same for all three activated Mo/ZSM-5 catalysts (Supporting Information, Figure S20) and thus did not depend on Mo loading. Moreover, the rate of the isotopic exchange correlated with the progress of catalyst induction (Figure 4b; Supporting Information, Figures S21, S22). This trend clearly underlines the important catalytic role of the confined carbon species. Another finding supporting this conclusion is that removal of the confined carbon molecules by hydrogenation restores the induction period, when methane is subsequently pulsed to the catalyst (Figure 5). Together with the isotope labelling data, these

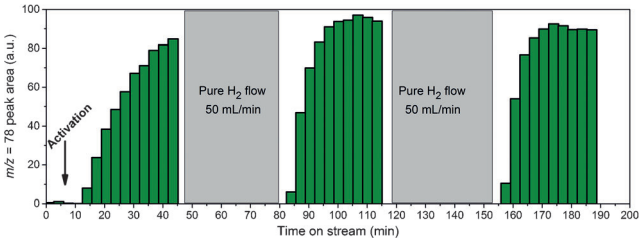

Figure 5. Integrated areas of MS $m/z=78$ peaks recorded during cycling pulse operation of the 2%Mo with methane pulses and subsequent hydrogenation of surface species by a continuous hydrogen flow at 700°C. Corresponding MS profiles are shown in the Supporting Information, Figure S23.

results unambiguously confirm that the hydrocarbons, confined in the zeolite pores, do not only participate in the MDA catalytic cycle but are also necessary for the production of aromatics. Also after removal of these species by hydrogenation, there is no activation period. This observation is consistent with the activation step pertaining to reduction of the Mo-phase and the induction step to formation of organocatalytic centers.

On the basis of the presented data, we infer that the mechanism by which methane is transformed into benzene is much more complex than anticipated. The novel aspect demonstrated in this work is that confined carbonaceous species are essential to the conversion of methane to benzene and hydrogen. We propose that the MDA reaction involves activation of methane over atomically dispersed Mo centers, anchored to the zeolite framework, producing reactive radicals or primary coupled C_2H_x fragments that react with polyaromatic hydrocarbon species confined in the pores of ZSM-5 zeolite and occupying at least 10–15% of the microporous space. We speculate that among the condensed aromatics that can be formed in the micropores of ZSM-5 zeolite (Supporting Information, Figures S24–S29), linear acenes are of particular interest, because they become increasingly unstable when more aromatic rings are added.[19] Hydrogenolysis of acenes may take place, resulting in the formation of benzene and other light aromatics (Figure 4c). Moreover, as EPR shows that radicals are formed in the process, the MDA reaction may have similarities with the mechanism underlying high-temperature non-oxidative conversion of methane over single-site Fe catalysts, as explored by Bao and co-workers.[20]

Finally, it is important to mention that the reported mechanistic findings possess some similarity to the well-established methanol-to-hydrocarbons (MTH) mechanism in which also an organocatalytic intermediate features. We contend that there are also differences. While the MTH reaction takes place via carbocation chemistry, the MDA reaction most likely involves radicals. Overall, the indications regarding the role of confined carbon species in the MDA

reaction mechanism should be taken as a valuable starting point for further investigations. Elucidation of the exact nature and chemistry of the hydrocarbon intermediates involved in the MDA reaction may contribute to developing more active and stable MDA catalysts.

Acknowledgements

Financial support from the SABIC-NWO CATC1CHEM CHIPP project is gratefully acknowledged. M.V.F. would like to thank the Russian Science Foundation (14-13-00826) for supporting the EPR studies. A.S.P. would like to thank FASO (0333-2016-0001). The authors thank Dr. Frans Tichelaar (TU Delft) for assistance with TEM analysis and Dr. Alessandro Longo for assistance with XAS experiments. We thank Dr. Christoph Dittrich (SABIC), Dr. Frank Mostert (SABIC), Dr. Xander Nijhuis (SABIC), Prof. Dr. Freek Kapteijn (TU Delft), Prof. Dr. Jorge Gascon (TU Delft), and Ina Vollmer (TU Delft) for fruitful discussion. We thank Kira Vranken for the design of cover image.

Conflict of interest

The authors declare no conflict of interest.

Keywords: organocatalysis · dehydroaromatization · hydrocarbons · methane · Mo/ZSM-5

[1] E. McFarland, *Science* **2012**, *338*, 340 – 342.
[2] a) A. I. Olivos Suarez, Á. Szécsényi, E. J. M. Hensen, J. Ruiz-Martínez, E. A. Pidko, J. Gascon, *ACS Catal.* **2016**, *6*, 2965 – 2981; b) M. Bordeaux, A. Galarneau, J. Drone, *Angew. Chem. Int. Ed.* **2012**, *51*, 10712 – 10723; *Angew. Chem.* **2012**, *124*, 10870 – 10881.
[3] O. V. Bragin, T. V. Vasina, A. V. Preobrazhenskii, K. M. Minachev, *Bull. Acad. Sci. USSR Div. Chem. Sci.* **1989**, *38*, 680 – 680.
[4] a) Z. R. Ismagilov, E. V. Matus, L. T. Tsikoza, *Energy Environ. Sci.* **2008**, *1*, 526 – 541; b) P. Schwach, X. Pan, X. Bao, *Chem. Rev.* **2017**, *117*, 8497 – 8520.
[5] a) D. Ma, Y. Shu, M. Cheng, Y. Xu, X. Bao, *J. Catal.* **2000**, *194*, 105 – 114; b) D. Ma, D. Wang, L. Su, Y. Shu, Y. Xu, X. Bao, *J. Catal.* **2002**, *208*, 260 – 269; c) J. Xue, Y. Chen, Y. Wei, A. Feldhoff, H. Wang, J. Caro, *ACS Catal.* **2016**, *6*, 2448 – 2451.
[6] a) Z. Cao, H. Jiang, H. Luo, S. Baumann, W. A. Meulenberg, J. Assmann, L. Mleczko, Y. Liu, J. Caro, *Angew. Chem. Int. Ed.* **2013**, *52*, 13794 – 13797; *Angew. Chem.* **2013**, *125*, 14039 – 14042; b) S. H. Morejudo, et al., *Science* **2016**, *353*, 563 – 566; c) N. Kosinov, F. J. A. G. Coumans, E. Uslamin, F. Kapteijn, E. J. M. Hensen, *Angew. Chem. Int. Ed.* **2016**, *55*, 15086 – 15090; *Angew. Chem.* **2016**, *128*, 15310 – 15314.
[7] a) D. Ma, W. Zhang, Y. Shu, X. Liu, Y. Xu, X. Bao, *Catal. Lett.* **2000**, *66*, 155 – 160; b) H. Liu, W. Shen, X. Bao, Y. Xu, *Appl. Catal. A* **2005**, *295*, 79 – 88; c) H. Zheng, D. Ma, X. Bao, Z. H. Jian, H. K. Ja, Y. Wang, C. H. F. Peden, *J. Am. Chem. Soc.* **2008**, *130*, 3722 – 3723; d) J. Gao, Y. Zheng, J.-M. Jehng, Y. Tang, I. E. Wachs, S. G. Podkolzin, *Science* **2015**, *348*, 686 – 690.
[8] N. Kosinov, F. J. A. G. Coumans, E. A. Uslamin, A. S. G. Wijpkema, B. Mezari, E. J. M. Hensen, *ACS Catal.* **2017**, *7*, 520 – 529.
[9] W. Song, H. Fu, J. F. Haw, *J. Am. Chem. Soc.* **2001**, *123*, 4749 – 4754.
[10] N. Kosinov, F. J. A. G. Coumans, G. Li, E. Uslamin, B. Mezari, A. S. G. Wijpkema, E. A. Pidko, E. J. M. Hensen, *J. Catal.* **2017**, *346*, 125 – 133.
[11] I. Lezcano-González, R. Oord, M. Rovezzi, P. Glatzel, S. W. Botchway, B. M. Weckhuysen, A. M. Beale, *Angew. Chem. Int. Ed.* **2016**, *55*, 5215 – 5219; *Angew. Chem.* **2016**, *128*, 5301 – 5305.
[12] a) C. H. Collett, J. Mcgregor, *Catal. Sci. Technol.* **2016**, *6*, 363 – 378; b) U. Olsbye, et al., *Angew. Chem. Int. Ed.* **2012**, *51*, 5810 – 5831; *Angew. Chem.* **2012**, *124*, 5910 – 5933; c) J. McGregor, et al., *J. Catal.* **2010**, *269*, 329 – 339.
[13] a) H. Jiang, L. Wang, W. Cui, Y. Xu, *Catal. Lett.* **1999**, *57*, 95 – 102; b) Y. H. Kim, R. W. Borry, E. Iglesia, *Microporous Mesoporous Mater.* **2000**, *35 – 36*, 495 – 509.
[14] H. G. Jang, H. K. Min, S. B. Hong, G. Seo, *J. Catal.* **2013**, *299*, 240 – 248.
[15] L. Li, X.-S. Zhou, G.-D. Li, X.-L. Pan, J.-S. Chen, *Angew. Chem. Int. Ed.* **2009**, *48*, 6678 – 6682; *Angew. Chem.* **2009**, *121*, 6806 – 6810.
[16] D. Ma, Y. Shu, X. Bao, Y. Xu, *J. Catal.* **2000**, *189*, 314 – 325.
[17] K. Kim, et al., *Nature* **2016**, *535*, 131 – 135.
[18] T. Xiao, et al., *J. Mater. Chem.* **2001**, *11*, 3094 – 3098.
[19] a) J. E. Anthony, *Angew. Chem. Int. Ed.* **2008**, *47*, 452 – 483; *Angew. Chem.* **2008**, *120*, 460 – 492.
[20] a) X. Guo, et al., *Science* **2014**, *344*, 616 – 619.

Manuscript received: October 29, 2017
Revised manuscript received: November 25, 2017
Accepted manuscript online: November 27, 2017
Version of record online: ■■ ■■, ■■■■

Zuschriften

Zeolithe

N. Kosinov,* A. S. G. Wijpkema, E. Uslamin, R. Rohling, F. J. A. G. Coumans, B. Mezari, A. Parastaev, A. S. Poryvaev, M. V. Fedin, E. A. Pidko, E. J. M. Hensen* _____ ▮▮▮▮–▮▮▮▮

Confined Carbon Mediating Dehydroaromatization of Methane over Mo/ZSM-5

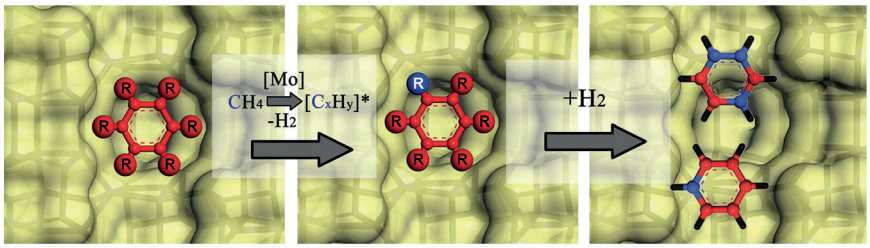

Pulsreaktionstechniken, Spektroskopie, Mikroskopie und Isotopenmarkierung wurden zur Charakterisierung des Zeoliths Mo/ZSM-5 einsetzt. Es zeigt sich, dass ein Kohlenwasserstoff-Pool aus Polyarenen innerhalb der Zeolithporen an der Aromatisierung von Methan über Mo/ZSM-5-Ein-Zentren-Katalysatoren beteiligt ist.